

- (11) A. Ziabicki, Reports of the Institute of Fundamental Technological Research, Polish Academy of Sciences, No. 60, Warsaw, 1977.
- (12) K. Kobayashi and T. Nagasawa, *J. Macromol. Sci., Phys.*, **4**, 331 (1970).
- (13) W. R. Krigbaum and R. J. Roe, *J. Polym. Sci., Part A*, **2**, 4391 (1964).
- (14) W. J. Dunning, *Trans. Faraday Soc.*, **50**, 1155 (1954).
- (15) L. Jarecki, Reports of the Institute of Fundamental Technological Research, Polish Academy of Sciences, No. 26, Warsaw, 1974.
- (16) R. J. Roe and W. R. Krigbaum, *J. Appl. Phys.*, **35**, 2215 (1964).
- (17) T. Hashimoto, K. Nagatoshi, A. Todo, H. Hasegawa, and H. Kawai, *Macromolecules*, **7**, 364 (1974).

Distortions of Band Shapes in External Reflection Infrared Spectra of Thin Polymer Films on Metal Substrates

D. L. Allara,* A. Baca, and C. A. Pryde

Bell Laboratories, Murray Hill, New Jersey 07974. Received April 10, 1978

ABSTRACT: Films of poly(methyl methacrylate), of varying thicknesses from near monolayer to 2 μm , on gold and silicon substrates have been examined by external reflection infrared spectroscopy. The shape of the 1731 cm^{-1} C=O band has been determined as a function of film thickness, angle of incidence, and polarization of the incident beam. Theoretical calculations of the band shape distortions of the C=O stretching mode are in good agreement with the observed spectra. Additional calculations, based on indices of refraction calculated from the Kramers–Kronig relation, demonstrate the effects of wavelength, extinction coefficient, and bandwidth on hypothetical reflection spectra. Some general conclusions are drawn with respect to the types of shifts and distortions one can expect in the reflection spectra of typical organic polymer films. These results suggest that significant care be taken in the assessment of chemical changes from band shifts and splitting in polymer/metal reflection spectra.

I. Introduction

The need often arises, in both fundamental and practical studies, to obtain an infrared spectrum of a thin film on a reflective metal substrate. The use of transmission spectroscopy is effectively precluded by the high absorptivity of the metal. Therefore, spectra must be obtained by internal and/or external reflection techniques (IRS and ERS,¹⁴ respectively). These techniques are not as straightforward experimentally as transmission and problems often arise in quantitative interpretation because reflection spectra may be distorted relative to transmission with significant changes occurring in peak maxima. The physical basis for such distortion involves the significant contribution of the refractive index to the reflectivity of a sample coupled with the rapid changes in the refractive index in the region of an absorption band (the anomalous dispersion). Such effects are of importance, for example, in understanding the chemical and structural nature of thin films by the interpretation of spectral shifts relative to bulk transmission bands. Detailed descriptions of these phenomena, with examples, are given by Harrick² for IRS.

Optical effects must also be taken into account in the accurate interpretation of ERS,² but few examples quantitatively relating theory and experiment are available. Greenler, Rahn, and Schwartz¹ have experimentally obtained reflection spectra of Cu_2O films on Cu for thicknesses of Cu_2O between 450 and 4200 Å. The 623- cm^{-1} transmission band is shifted to 655 cm^{-1} in the multiple reflection mode with angles of incidence between 84 and 90°. Using theory based on classical physical optics and developed to a great extent in an earlier paper³ these authors calculated a band shift of 28 cm^{-1} and indicated that further correction of the calculations for small transmission shifts could improve the agreement. However, band splitting predicted by the calculations for 4200 to 12000 Å films was not observed in the experiments and thus some question remains regarding discrepancies be-

tween the experiment and theory over a wide range of thickness for typical experimental conditions. Calculations (but no experiments) were also made for copper surfaces with films of benzene, a weak absorber relative to Cu_2O (extinction coefficient of ~ 0.07 vs. ~ 5 , respectively). No shifts were predicted from these calculations. Therefore, these authors made the general and potentially useful conclusion that ERS (or RA¹⁴) spectra of "typical moderately strong infrared bands should be directly comparable with the transmission experiment."

Unfortunately, no other studies are available and some gaps between theory and experiment in ERS still exist. It was of particular importance to us to know whether band distortion effects would arise in organic polymer films (e.g., common metal coating materials) which contained absorbing groups intermediate in extinction coefficients between benzene and Cu_2O and, if so, whether these effects could be exactly calculable from the same theory that was only partially successful for Cu_2O films.¹ For this study, we chose poly(methyl methacrylate) (PMMA), a typical organic material with a distinct C=O stretching band at 1731 cm^{-1} . Films with thicknesses from near monolayer dimensions to 2 μm were prepared on gold substrates and several angles of incidence were used to give typical experimental conditions which spectroscopists might use. In addition, one experiment on a silicon substrate was done to examine the effect of a reflective dielectric material. Using our experimental results as a guide, calculations based on theory were carried out for hypothetical bands at 1000, 1731, and 3000 cm^{-1} to check the effects of variations in index of refraction, extinction coefficient, and wavelength on band distortions. Some useful generalizations are drawn from the experimental and calculated results in the last section. The results and conclusions should be broadly applicable to a variety of organic films and metals because most organic materials have very similar values of refractive indices (near 1.5 in nonab-

sorbing regions) and for highly reflective metal substrates, the spectrum of the organic film is nearly independent of the metal. It is not the purpose of this paper to present the optical theory in detail. Rather a brief description with appropriate references is given to describe the calculation methods and to provide a physical basis for qualitatively exploring the phenomena.

II. Experimental Section

1. Films. Films of PMMA, obtained both as commercial samples and polymer prepared in this laboratory, on gold and silicon substrates were prepared by spin coating from chlorobenzene solution. The substrates were placed horizontally on a spinning platform, flooded with polymer solution, and spun at speeds between 500 and 4000 rpm to give a uniform film. Excess solvent entrapped in the films was removed by heating in vacuo at a temperature just above the glass transition. The substrates consisted of 1.5–2-in. diameter optically polished silicon plates (surface roughness within ~ 50 Å), uncoated or coated with ~ 2000 Å of vapor deposited gold (99.99%). The thicknesses of the polymer layers were determined by ellipsometry at 633 nm. For films thicker than several thousand angstroms, measurements were also made using a Sloan Dektak surface profiler. For the latter measurement a sharp knife edge was used to chip out a portion of the film to leave bare substrate surface and the step height then was measured at several locations. As a general rule the film thickness measurement appeared to be accurate to within ± 100 Å for films thicker than several thousand angstroms. For thinner films more care was taken in the measurements and for films several hundred angstroms or less the errors were estimated to be ca. ± 20 Å on the average. Ellipsometer measurements showed that spot-to-spot variation of the thickness across the single surface was negligible in the thin films (1-mm resolution). Scanning electron microscopy and ESCA analysis of thin PMMA films on Si substrates, prepared as described above for Au, show no evidence for nonuniformity or pinholes.⁴

2. Sample Spectra. Single reflection spectra of the 1730–1732- cm^{-1} methacrylate C=O stretching band were obtained using a Perkin-Elmer 621 grating spectrometer for films >0.5 μm and a Digilab 15B Fourier transform interferometer system for the thin films. Both instruments were equipped with Perkin-Elmer wire grid polarizers and reflection optics designed by Harrick Scientific, which were somewhat modified for our purposes. A description of the single reflection apparatus has been previously reported.⁵ The average resolution of the spectrometers was ≤ 2 cm^{-1} under the conditions of our experiments. The angle of incidence can be set reproducibly to within ca. $\pm 0.5^\circ$. For the thick films the maximum beam spread is $\pm 6^\circ$. For the very thin films the beam was apertured down to a 2-mm diameter with a resultant approximate beam spread of $\pm 1^\circ$ and large numbers of scans were signal averaged to obtain accurate reflectivity ratios. The overall reflectivity of the reflecting optics including the sample was generally between 35 and 45%.

3. Optical Constants. For the theoretical band shape calculations based on the exact optical relationships given in the next section, it was necessary to evaluate the complex refractive index, $\hat{n}(\tilde{\nu})$, of PMMA as a function of frequency over the region 1650 to 1800 cm^{-1} . This section describes how \hat{n} was determined. The definition is given in eq 1, where n is the real refractive index and

$$\hat{n}(\tilde{\nu}) = n(\tilde{\nu}) + ik(\tilde{\nu}) \quad (1)$$

k is the attenuation constant, with both quantities written as functions of $\tilde{\nu}$ to show their dependence on frequency. Since conveniently measurable optical properties of a material such as reflectivity or transmissivity are functions of both n and k , two independent measurements under different conditions are needed to evaluate n and k experimentally at a specific frequency. The equations given in the next section which govern the exact relationship between n and k and the measured quantity such as reflectivity (R) or transmissivity (T) normally are written in terms of R and T as functions of n and k . Unfortunately, analytical expressions of n and k as functions of R and T are not easily derived under the conditions of most experiments. Therefore, calculation of n and k from experimental results must be done by reiterative, numerical computations and a reasonably accurate

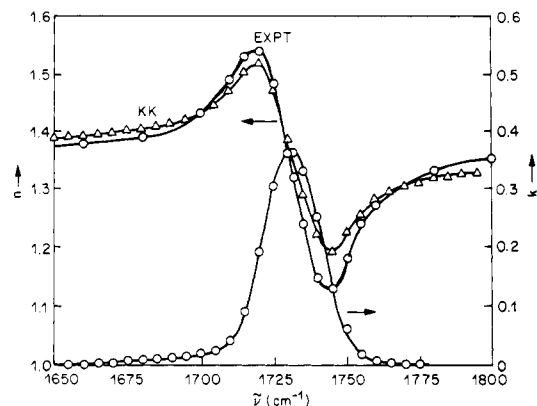


Figure 1. Plot of k and n vs. wavenumber for the PMMA C=O stretching band at 1731 cm^{-1} : O, experimental; Δ , Kramers-Kronig calculated values of n .

initial guess for n and/or k may be needed to achieve efficient convergence on the true solution. The transmission experiment at normal incidence provides a simple means of approximating k since this measurement is fairly insensitive (as a first approximation) to the value of n and the approximate relationship holds:

$$I/I_0 = e^{-4\pi k d \tilde{\nu}} \quad (2)$$

In eq 2 I/I_0 = fraction of power transmitted through the sample, d = film thickness, and $\tilde{\nu}$ = vacuum frequency in wave numbers. Applying eq 2 to transmission experiments with PMMA films of known thickness on NaCl and Si substrates approximate values of k were calculated. Using these k 's as initial guesses approximate values of n were obtained in two ways:

1. The reflection band of a bulk sample of PMMA was measured at a 70° angle of incidence and the ratio of reflectivities of p and s polarization (polarization conventions as shown in Figure 2) calculated. Using a computer program to obtain exact numerical solutions of the optical equations (next section), values of n were determined which satisfied the equations for the experimental R_p/R_s ratio and the trial k .

2. A numerical solution of the Kramers-Kronig (KK) relation (eq 3) between n and k was carried out with a computer. Equation

$$n(\nu_0) = n_\infty + \frac{1}{\pi} \int_{\nu_1}^{\nu_2} \frac{\nu^2 k(\nu) d\nu}{(\nu - \nu_0)} \quad (3)$$

3 is an approximation to the exact relation⁶ based on the assumptions that (1) the C=O vibration can be modeled as an isolated oscillator and (2) in the range of frequencies included in the absorption band, ν_1 to ν_2 , $\nu \gg (\nu - \nu_0)$ where ν_0 is the frequency at which n is evaluated. The term n_∞ represents the contribution of all other oscillators in the solid to the value of n and was evaluated experimentally at 1900 cm^{-1} by measurement of the critical angle for a KRS-5 hemispherical optical element coated with a several micron film of PMMA.⁷

Finally, the approximate n values were then applied as guesses to the exact equations (next section) for the transmission experiment (in which corrections are made for small reflection losses and interference effects) and significantly improved values of k obtained relative to those initially obtained from eq 2. More accurate values of n were then obtained from the bulk reflection experiment or the KK calculation. Further iterations of the process were run until convergence for n and k occurred. Normally two iterations were sufficient to give values of k and n which were stable within a few percent. The results are given in Figure 1.

In later sections values of n obtained from bulk PMMA reflection spectra are referred to as "experimental" and those from the Kramers-Kronig relation (eq 3) as KK values.

For gold, values of $n = 9.5$ and $k = 30$ were interpolated from recent data of Hagemann, Gudat, and Kunz.⁸ For silicon, standard values of $n = 3.418$, $k = 0$ were used. In general, the reflectivity calculations were not sensitive to small variations in the n and k values for gold and calculations based on other commonly accepted, earlier values of n and k are insignificantly different from current calculations (e.g., see ref 9).

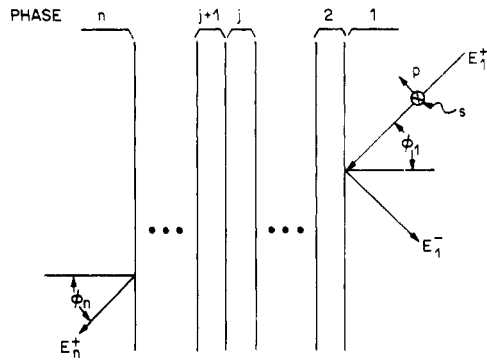


Figure 2. Physical description of the multilayered optical sample showing incoming and outgoing beams of light and defining the angles of incidence, polarization states, and indexing of layers.

III. Theory and Physical Basis for Band Distortions

In order to carry out accurate band shape calculations it is necessary to define the exact relationship between the reflectivity and transmissivity of a multilayer sample and the angle of incidence, polarization, and wavelength of the incident radiation and optical constants of all components of the system.

The theory used is based on the boundary value solutions of the classical electromagnetic equations for the interaction of a propagating infinite plane wave with a system of parallel, optically isotropic layers whose optical properties are completely described by the complex refractive index. This theory is generally accepted as rigorously correct with the assumptions stated above. General formulations of these equations have been treated elsewhere¹⁰ and specific treatments of general use in reflection spectroscopy have been discussed by several workers including Greenler,³ McIntyre,¹¹ and Hansen.¹² The discussion of the equations below assumes the reader has a basic knowledge of the optics of stratified layers.¹⁰ The qualitative discussion that follows does not.

The equations for transmission and reflection of multiphase systems (Figure 2) were set up as follows¹⁰ and numerical solutions were implemented on a Honeywell 6000 computer. The development of the equations is straightforward and further details can be found in ref 10. The fractions of power transmitted (T) and reflected (R), for parallel or perpendicular polarization, are defined by eq 4 and 5 in terms of the overall complex Fresnel coef-

$$T = \frac{n_n}{n_1} t t^* \quad (4)$$

$$R = r r^* \quad (5)$$

ficients t and r , defined below (an asterisk represents the complex conjugate). The n 's are the refractive indices of the initial and final phases. These equations are readily evaluated in an n -phase system by the well-known matrix relations

$$M = \prod_{j=2}^n C_j$$

where

$$C_j = \begin{bmatrix} e^{-i\delta_{j-1}} & r_j e^{-i\delta_{j-1}} \\ r_j e^{i\delta_{j-1}} & e^{i\delta_{j-1}} \end{bmatrix}$$

in which the phase angle term $\delta_j = (2n/\lambda) \hat{n}_j d_j \cos \phi_j$ for angle of incidence ϕ_j and vacuum wavelength λ and r_j = the Fresnel reflection coefficient for the boundary between phases $j-1$ and j . The matrix elements of M can be

evaluated from the optical constants and experimental parameters and then t and r can be calculated from

$$t = \left(\prod_{j=2}^n t_j \right) m_{11} = E_n^+ / E_1^+$$

and

$$r = m_{21} / m_{11} = E_1^- / E_1^+$$

where t_j = the Fresnel transmission coefficient for the boundary of phases $j-1$ and j and the electric field terms $E_1^{+(-)}$ are defined in Figure 2. The exact forms of the Fresnel coefficients in terms of the \hat{n} 's, ϕ_1 , and λ can be readily obtained elsewhere.¹⁰⁻¹²

The final calculation of R or T for a specific polarization is carried out by using the appropriate form of the Fresnel coefficients for parallel (p) or perpendicular (s) polarization.¹⁰

The exact forms of the above equations varied according to application, two or three phases for reflection or unsupported film experiments and four for supported film transmission.

The theory allows a qualitative description of distortion effects in reflection spectra.² The following discussion is only meant to roughly gauge the types of effects possible. A complete analysis of the contributing physical factors in a reflection spectrum is quite complex and not always possible.^{11,12} The incoming and reflected rays of light are not necessarily in phase at the surface of the metal and the size of the phase shift determines the magnitude of the net electric field at the surfaces. A finite value of the electric field is required for interaction with an oscillator and the resultant energy absorption. Detailed descriptions for the IR are given by Greenler.³ The value of the phase shift depends upon the angle of incidence and the optical constants of the system. For example, for p polarization, glancing angles of incidence give rise to large surface fields. As a result, monolayer or ultrathin film spectra can be observed under these conditions, whereas other angles and/or polarization give near zero fields and do not give rise to spectra of thin films. The electric field at the surface is part of a standing wave which extends above the surface. For a weakly absorbing medium the field varies periodically into the adjacent medium (film) with a repeat distance, $d' = (2\bar{n} \cos \phi)^{-1}$ where ϕ is the angle of incidence at the metal surface and \bar{n} is the refractive index of the film. It can readily be seen that for different regions of frequency of an absorption band the value of d' will differ because of different values of \bar{n} observed in the anomalous dispersion curve (Figure 1). It follows that the electric fields at any fixed distance from the surface will differ (periodic variations are different) for different frequency regions of the band and the net amount of energy absorption will be controlled not only by k but by \bar{n} . Thus opposite sides of a reflection band will in general be asymmetric. It also follows that distortion effects will change faster with increasing film thickness when ϕ is smaller (near normal incidences) and when \bar{n} is large.

Another underlying effect in band distortion involves reflection of a fraction of the incoming beam off the front surface of the film (rather than the metal substrate surface). This component of the reflection, for constant or negligible values of k , should increase with increasing values of \bar{n} . In the low region of \bar{n} (high frequency) in the dispersion curve (Figure 1) less light will be reflected from the front surface than in the high region of \bar{n} . Thus the reflection band will be distorted somewhat by this effect and the distortion will cause a shift toward higher frequencies. In addition, for a particular combination of \bar{n} , n , and ϕ there exist a minimum thickness and integral

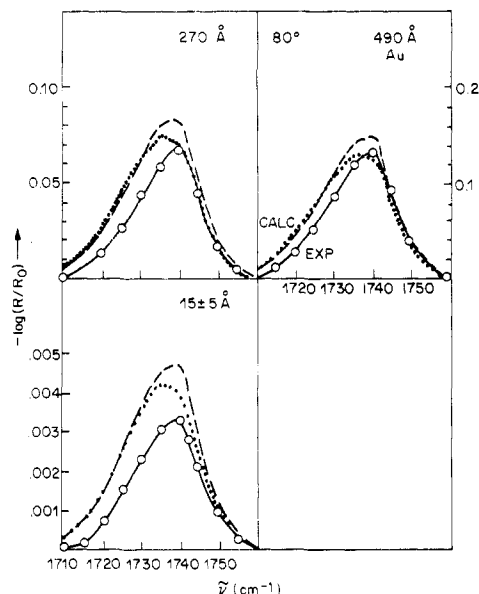


Figure 3. Band shapes for PMMA films on gold at an 80° angle of incidence and p polarization: ○, experimental curves; ---, calculated curves based on experimental n ; ···, calculated curves based on KK n .

multiples thereof which give rise to an interference between reflected waves from the substrate metal and the film surface and which result in a loss in reflectivity. These spikes will arise at different thicknesses for different portions of the band and give rise to distortions. The thickness for the first appearance of the interference is a fraction of the wavelength for typical angles of incidence.² In physical reality all of these effects are coupled and it is difficult to actually separate them quantitatively into discrete contributions. The net result of these effects can be observed in reflection spectra and are useful in qualitatively understanding the nature of the spectra in the following sections. The complete physical blending and interaction of all these effects, however, are taken into account in the numerical calculations from the theory.

IV. Results and Discussion

1. The 1731-cm⁻¹ PMMA Band. a. Thin Films, ≤1000 Å. For thin films, particularly those of near-monolayer thicknesses, p polarization and angles of incidence near glancing are necessary for optimum absorption^{3,13} (see earlier section).

Experimental and calculated band shapes for films on gold substrates with p polarization are given in Figure 3 for gold substrates with 15, 270, and 490 Å films at an 80° angle of incidence and in Figure 4 for a 650 Å film at 82°. The intensities and overall band shapes closely agree except for the calculated band maxima which exhibit broad tops. The transmission maximum occurs at 1731 to 1732 cm⁻¹ in contrast to the reflection results in Figures 3 and 4 which show $\nu_{\text{max}} \sim 1740$ cm⁻¹ (except for the KK based calculation).

This shift of 8–10 cm⁻¹ in the near monolayer, submicron films thus can be assigned to optical effects. The broader “flat-topped” appearance of the calculation based on the KK values of n , relative to the calculation based on experimental values of n , can be correlated with the less severe dip in n in the region around 1740 cm⁻¹ in the anomalous dispersion curve of the KK curve in Figure 1. This result should be fairly general because the anomalous dispersion curve, for reasonably symmetrical bands, always has the same general features and, therefore, monolayer and ultrathin film reflection spectra should always show

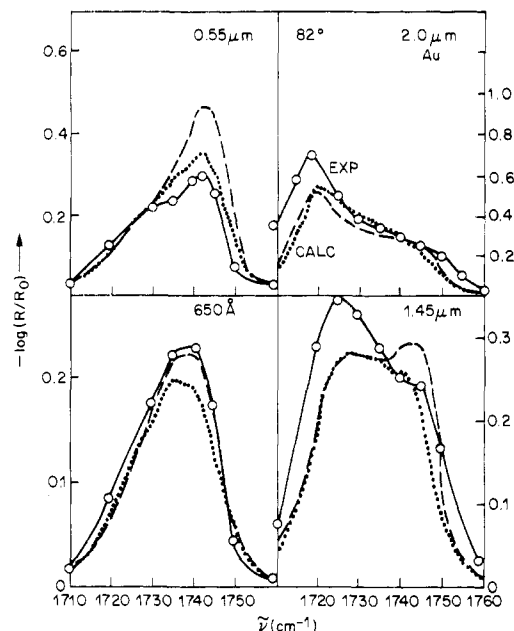


Figure 4. Band shapes for PMMA films on gold at an 82° angle of incidence and p polarization: ○, experimental curves; ---, calculated curves based on experimental n ; ···, calculated curves based on KK n .

peak maximum shifts to higher frequencies than transmission.

One experiment was carried out with a 540-Å film on a silicon substrate and the result is given in Figure 5. Note that the band represents a net power gain (band upside down or negative absorbance) and this is predicted by the theoretical calculations. Normally transmission or IRS spectra would be used for silicon substrates (where the sample physically permits). However, when ERS is used with materials of low k (dielectric or nonmetals) one must be aware of the possibility of band inversions (see also ref 11). Such inversions should not preclude quantitative studies since the general theory is applicable but note that agreement in Figure 5 is not as close as in the gold substrate samples.

b. Thick Films. As the film thickness increases to the micron region the distortion of the absorption band at glancing angles becomes quite severe as shown in Figure 4. The calculated results describe the observed overall band shapes and intensities fairly well except for the 1.45-μm film where the calculations correctly indicate band splitting but over emphasize the high-frequency shoulder. It is instructive to note that a new species is not associated with this band splitting but rather the same oscillator group is responsible for both peaks. With films thousands of angstroms thick, intense spectra can be obtained at nonglancing and even near-normal angles of incidence with either p or s polarization (the E fields become large at these distances for the above conditions) and it is usually experimentally more convenient to work at some intermediate angle such as 45° with unpolarized light. Calculated and observed spectra for nonglancing angles and p polarization are shown in Figures 6 and 7. Again, the bands are distorted. The observed distortion features, shoulders and shifted peak maxima, are generally predicted by the calculations. The results with s polarized or unpolarized light are similar in that distortions are observed and can be predicted from theory as accurately as with the given p polarization examples. For brevity these results are not shown. The thicknesses of these films are in the region (one to several μm) where interference effects begin to take place and some of the sharp “spiking” in the spectra could

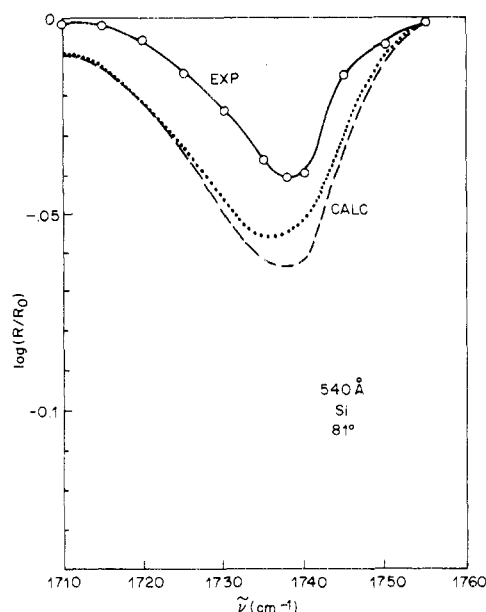


Figure 5. Band shapes for a 540-Å PMMA film on silicon at an 81° angle of incidence and p polarization: O, experimental curve; ---, calculated curve for experimental n ; ···, calculated curve for KK n .

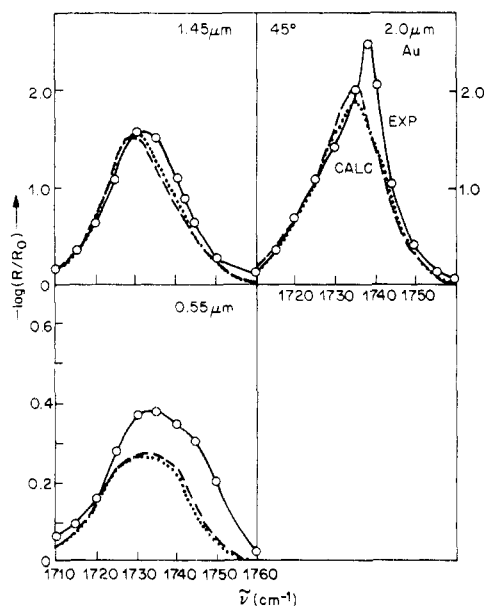


Figure 6. Band shapes for PMMA films on gold at a 45° angle of incidence and p polarization: O, experimental curve; ---, calculated curves for experimental n ; ···, calculated curves for KK n .

be attributable to these effects.

2. Effects of \hat{n} and ν on Calculated Band Shapes.

It is of considerable practical importance to be able to predict whether large distortion effects in IR reflection spectra will occur with a given type of sample for given conditions. Greenler, Rahn, and Schwartz¹ previously indicated little distortion for $k \sim 5$ (the 609 cm^{-1} Cu_2O band, $\sim 30 \text{ cm}^{-1}$ shift). The distortion is obviously a function of both n and k but n is a function of k via the Kramers-Kronig relation⁵ (eq 3). This allows qualitative generalizations to be made in terms of k , which can be easily estimated whenever a well-defined, quantitative transmission spectrum can be obtained (eq 2) for the band of interest.

Calculations were carried out for hypothetical $\text{C}=\text{O}$ stretching bands with $\bar{\nu}_{\text{max}} = 1732 \text{ cm}^{-1}$ with various

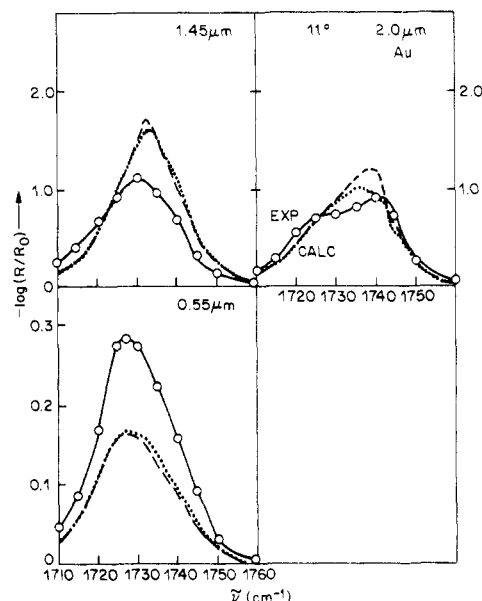


Figure 7. Band shapes for PMMA films on gold at an 11° angle of incidence and p polarization: O, experimental curve; ---, calculated curve for experimental n ; ···, calculated curve for KK n .

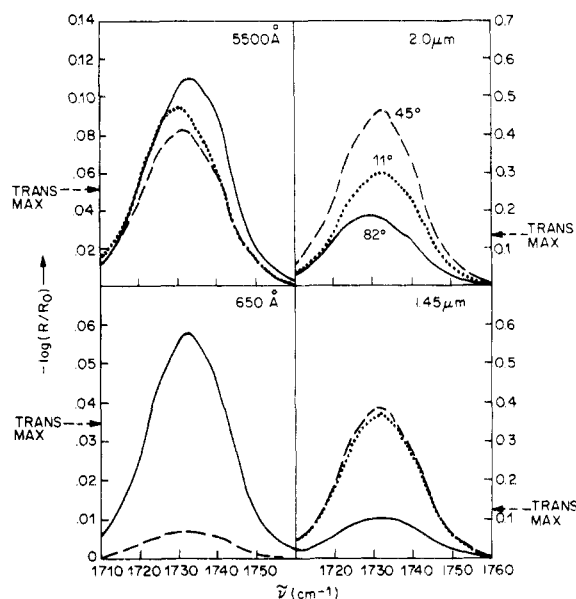


Figure 8. Calculated band shapes for hypothetical films on gold with $k_{\text{max}} = 0.1$, $\nu_{1/2} = 12 \text{ cm}^{-1}$, and p polarization: —, 82° angle of incidence; ---, 45° angle of incidence; ···, 11° angle of incidence.

distributions $k(\bar{\nu})$. Using eq 3, $n(\bar{\nu})$ curves were computed and then theoretical reflection spectra were generated under conditions used in Figures 3–7. The distribution of k in Figure 1 is approximately Gaussian (a Lorentzian distribution is much too broad to fit the data) with a half-width of $\bar{\nu}_{1/2} = 12 \text{ cm}^{-1}$. The results of these calculations are as follows: (1) For a fixed value of $k_{\text{max}} \sim 0.4$ (for PMMA $k_{\text{max}} = 0.36$) increasing the half-width from the PMMA value of 12 cm^{-1} gives larger and correspondingly broader $n(\bar{\nu})$ curves and broader distortions than PMMA. Conversely, for a sharper band, $\bar{\nu}_{1/2} = 6 \text{ cm}^{-1}$, the $n(\bar{\nu})$ is a sharper curve and the distortions are less, e.g., peak maxima shift within a range of $\sim 9 \text{ cm}^{-1}$ compared to 25 cm^{-1} in Figures 3–7. (2) If the value of k_{max} is reduced from 0.4 to 0.1 and the half-width kept at the PMMA value of 12 cm^{-1} , the extreme ν_{max} shifts are within the range of $\pm 2 \text{ cm}^{-1}$ over all conditions in Figures 3–7. These results are shown in Figure 8. For comparison

purposes, the plots in Figure 8 also show the calculated maximum absorbance values for transmission at normal incidence through the same films with substrates removed. The complete transmission bands would be symmetrical (close to Gaussian) around the maximum (except for minor distortions due to surface reflections).

Calculations also were carried out in which the $k(\bar{\nu})$ distribution for PMMA with $\bar{\nu}_{1/2} = 12 \text{ cm}^{-1}$ was used but the band center (maximum) was moved to 1000 and 3000 cm^{-1} to generate hypothetical bands at these two frequencies. The $n(\bar{\nu})$ curves were calculated from the KK relation. The results gave the same qualitative behavior as in Figures 3–7 for the 1731- cm^{-1} PMMA band but for the 3000- cm^{-1} band the distortion changes as functions of film thickness began to appear at lower film thicknesses than for the 1000- cm^{-1} band. Such an effect would be expected based on the periodic variation of field strength as a function of distance with a repeat distance proportional to $1/\bar{\nu}$ (see earlier section).

3. Conclusions and Some Generalizations. Generally good, but not precise, agreement is obtained between theory and experiment. It is most likely that the theory is quantitatively applicable and that the observed discrepancies are due to a combination of experimental errors in the reflection spectra and the measured optical constant data. Similar causes probably are responsible for the lack of observed band splitting in Greenler, Rahn, and Schwartz's earlier work on Cu_2O .¹ From a practical point of view, however, the present results are sufficiently accurate to allow a number of interesting conclusions.

The following useful generalizations can be made for the reflection spectrum of an organic substance with a reasonably isolated band in the mid-IR region for conditions of a range of incidence angles from a highly reflective substrate.

(1) For typical bands of $\nu_{1/2} \sim 20 \text{ cm}^{-1}$ and $k > 0.1$, significant distortions can occur with peak maxima shifting, relative to transmission spectra, several wavenumbers for the lower range up to tens of wavenumbers for $k \gg 0.1$ (e.g., Greenler, Rahn, and Schwartz,¹ $\sim 30\text{-cm}^{-1}$ shift¹ for $k \sim 5$).

(2) For sharp bands, $\nu_{1/2} \lesssim 5 \text{ cm}^{-1}$, the shifts are several times less than for the broad bands in (1) above for equivalent k_{max} and $\bar{\nu}_{\text{max}}$ values.

(3) For bands with $k < 0.1$, shifts and distortion are minimal and transmission and reflection spectra will be nearly identical within $\sim 1 \text{ cm}^{-1}$. It should be noted that while reflection band shapes are close to those of transmission (close to symmetrical) the intensities need not be close to hypothetical transmission values for a free-standing film, especially for reflection at glancing angles (see Figure 8) compared to transmission at normal incidence.

(4) In monolayer and very thin films at glancing angles of incidence, the reflection shifts will always be to higher

frequencies relative to the transmission maximum.

(5) For two bands with similar values of k_{max} and $\bar{\nu}_{1/2}$, reflection spectra will show nearly identical shifts for the same experimental conditions. However, as film thicknesses increase, distortion effects will change more rapidly for the higher frequency band.

Of practical concern is the generalization that typical strongly absorbing functional groups such as $\text{C}=\text{O}$, $\text{C}=\text{N}$, $\text{C}-\text{O}$, etc., incorporated into a polymer matrix in high concentrations (e.g., every repeat unit) can lead to shifts of significance in quantitative work. This paper shows that one can recognize when difficulties may arise and potentially correct for distortion when necessary.

Acknowledgment. The authors acknowledge helpful discussions with J. D. E. McIntyre and D. E. Aspnes. We are grateful to N. J. Harrick for originally pointing out the significance of optical effects and helpful suggestions in the early portion of this work.

References and Notes

- (1) R. G. Greenler, R. R. Rahn, and J. P. Schwartz, *J. Catal.*, **23**, 42 (1971).
- (2) N. J. Harrick in "Characterization of Metal and Polymer Surfaces", Vol. 2, L. H. Lee, Ed., Academic Press, New York, N.Y., 1977, pp 153–192.
- (3) R. G. Greenler, *J. Chem. Phys.*, **44**, 310 (1966).
- (4) D. L. Allara, C. A. Pryde, and R. F. Roberts, unpublished results.
- (5) H. G. Tompkins and D. L. Allara, *Rev. Sci. Instrum.*, **45**, 1221 (1974).
- (6) For example, F. Stern in "Solid State Physics, Advances in Research and Applications", Vol. 15, F. Seitz and D. Turnbull, Eds., Academic Press, New York, N.Y., 1963 pp 299–408.
- (7) A description of this method can be found in: N. J. Harrick, "Internal Reflection Spectroscopy", Wiley-Interscience, New York, N.Y., 1967.
- (8) H. Hageman, W. Gudat, and C. Kunz, *J. Opt. Soc. Am.*, **65**, 742 (1975).
- (9) R. G. Greenler, *J. Vac. Sci. Technol.*, **12**, 1410 (1975).
- (10) O. S. Heavens, "Optical Properties of Thin Solid Films", Dover Publications, New York, N.Y., 1965, Chapter 4; for a more recent general treatment, see also, e.g., D. W. Berreman, *J. Opt. Soc. Am.*, **62**, 502 (1972). For a thorough presentation of the principles see M. Born and E. Wolf, "Principles of Optics", 5th ed., Pergamon Press, New York, N.Y., 1975.
- (11) J. D. E. McIntyre in "Optical Properties of Solids, New Developments", B. O. Seraphin, Ed., American Elsevier, New York, N.Y., 1976, Chapter 11; and in "Advances in Electrochemistry and Electrochemical Engineering", Vol. 9, P. Delahay and C. W. Tobias, Eds., Wiley, New York, N.Y., 1973, pp 61–66 and references therein.
- (12) W. N. Hansen in "Progress in Nuclear Energy", Vol. 11, H. A. Elion and D. C. Steward, Eds., Chapter 1; and in "Advances in Electrochemistry and Electrochemical Engineering", Vol. 9, P. Delahay and C. W. Tobias, Eds., Wiley, New York, N.Y., 1973, pp 1–60 and references therein.
- (13) R. G. Greenler, *J. Chem. Phys.*, **50**, 1963 (1969).
- (14) Both the term reflection-absorption (RA) originated by Greenler et al.² and the term specular reflection have been used to denote external reflection. The RA term, which previously has been used by us, can be misleading in certain cases of dielectric substrates with strongly absorbing overlayers where reflection bands can have negative absorbances and represent increased reflectivities rather than absorption relative to the baseline.